

Composite Higgs Boson Pair Production at the LHC

R. Gröber^a and M. Mühlleitner^a

^a*Institut für Theoretische Physik, Karlsruhe Institute of Technology, 76128 Karlsruhe, Germany*

Abstract

The measurement of the trilinear and quartic Higgs self-couplings is necessary for the reconstruction of the Higgs potential. This way the Higgs mechanism as the origin of electroweak symmetry breaking can be tested. The couplings are accessible in multi-Higgs production processes at the LHC. In this paper we investigate the prospects of measuring the trilinear Higgs coupling in composite Higgs models. In these models, the Higgs boson emerges as a pseudo-Goldstone boson of a strongly interacting sector, and the Higgs potential is generated by loops of the Standard Model (SM) gauge bosons and fermions. The Higgs self-couplings are modified compared to the SM and controlled by the compositeness parameter ξ in addition to the Higgs boson mass. We construct areas of sensitivity to the trilinear Higgs coupling in the relevant parameter space for various final states.

1 Introduction

The Standard Model of particle physics has been extremely successful in describing the fundamental forces of the weak, electromagnetic and strong interactions. It is based on the $SU(2)_L \times U(1)_Y$ gauge group which is spontaneously broken down to the electromagnetic group $U(1)_{em}$. The electroweak symmetry breaking (EWSB) mechanism has been implemented in the most economical way by adding a single weak isodoublet scalar field [1–3]. Three of its four degrees of freedom, the pseudo-Nambu-Goldstone bosons, provide the masses of the massive electroweak gauge bosons, W^\pm and Z . The remaining physical degree of freedom is associated with the SM Higgs boson. Also the fermions acquire their masses through the interaction with the Higgs boson in the ground state. The non-vanishing vacuum expectation value, which is essential for the non-zero particle masses, is induced by the typical form of the Higgs potential. Since all the Higgs couplings are predetermined, the parameters describing the Higgs particle are entirely fixed by its mass. It is the only unknown parameter in the SM Higgs sector [3]. Furthermore, the Higgs boson plays the role of an ultraviolet moderator. It ensures unitarity in the scattering of massive longitudinal gauge bosons.

Despite the fact that no experimental evidence has been found so far for the Higgs mechanism, the SM is in very good agreement with electroweak precision tests at LEP, SLC, Tevatron and HERA. Any departure from the SM has to pass the test of EW precision measurements. Considering new physics beyond the minimal version of the SM Higgs hence motivates smooth departures from the SM. This is *i.e.* given by the introduction of a light Higgs boson which emerges as a pseudo-Goldstone boson from a strongly-coupled sector [4], the so-called Strongly Interacting Light Higgs (SILH) scenario [5, 6]. It is a bound state emerging from strong dynamics [7, 8], and due to its Goldstone nature it is separated by a mass gap from the other usual resonances of the strong sector. At low energy, the composite model therefore has the same particle content as in the SM, with a light and narrow Higgs-like scalar. Because of the composite nature its couplings, however, are different from the SM case. This can have significant impacts on the experimental sensitivities in the LHC Higgs boson search channels [5, 9, 10].

In Ref. [5] an effective Lagrangian for a composite light Higgs boson was constructed. It was shown that with respect to LHC studies the Higgs properties are described by its mass and two new parameters. The effective SILH Lagrangian represents the first term of the expansion in $\xi = (v/f)^2$ where $v = 1/\sqrt{2}G_F \approx 246$ GeV is the scale of EWSB and f is the strong dynamics scale. It describes the physics near the SM limit $\xi \rightarrow 0$, whereas in the technicolor limit [11], $\xi \rightarrow 1$, a resummation of the full series in ξ is needed. Such a resummation is provided for instance by explicit models built in five-dimensional warped space. In this paper we chose two five-dimensional models which we hope to be representative of minimal composite Higgs models. The deviations from the SM couplings are governed by only one parameter ξ which varies from 0 to 1. We did not take into account couplings with a different Lorentz structure. They are generated via the exchange of heavy resonances of the strong sector and suppressed by at least $(f/m_\rho)^2$, with $m_\rho > 2.5$ TeV being the typical scale of the heavy resonances. A direct Higgs coupling to two gluons or two photons will also always be sub-leading compared to the couplings considered in this paper. And the effect of new heavy top partners is already included in the effective Lagrangian approach [5, 9, 10, 12].

While the SM Higgs boson suffers from the hierarchy problem, this problem does not arise for a composite Higgs state. The Higgs potential vanishes at tree level due to the non-linear Goldstone

symmetry acting on it. However, the global symmetry of the strong sector is explicitly broken by the couplings of the SM fields to the strong sector. The Higgs potential is thus generated by loops of SM fermions and gauge bosons. The EWSB scale is dynamically generated and can be smaller than the scale f , in contrast to technicolor models where there is no separation of scales. The Higgs gets a light mass through loops with $m_h \sim g_{SM}v$ where $g_{SM} \lesssim 1$ is a generic SM coupling.

Although the composite Higgs boson couplings, deviating from the SM, are no direct probe of the strong sector at the origin of the electroweak symmetry breaking¹ their determination would allow for first insights in the dynamics controlling the Higgs sector. With the measurement of the Higgs self-couplings the Higgs potential can be reconstructed and thus the Higgs sector of EWSB can be tested. Furthermore, consistency tests within the framework of the considered model can be performed by comparing with the other Higgs couplings to fermions and gauge bosons. In this paper we focus on the determination of the trilinear composite Higgs self-coupling λ_{HHH} in order to investigate the prospects of testing the dynamics responsible for generating the Higgs potential. This coupling is accessible in Higgs pair production processes [14, 15]. In the SM the extraction of λ_{HHH} at the LHC is extremely challenging due to small cross sections and large backgrounds [16–18]. Our goal is to find parameter regions where λ_{HHH} might be accessible.² We hope this to motivate realistic analyses taking into account the relevant background processes and detector effects which is beyond the scope of our paper.

The organization of the paper is as follows. In section 2 we will introduce the Higgs potential and the general parametrization of the Higgs couplings. In section 3 the various Higgs pair production cross sections at the LHC will be analyzed. In section 4 we will present and discuss the sensitivity for the extraction of λ_{HHH} before we will conclude in section 5.

2 Higgs potential and parametrization of the Higgs couplings

The Holographic Higgs models of Refs. [20–22] which are based on a five-dimensional theory in Anti de-Sitter (AdS) space-time, provide a resummation in the compositeness parameter $\xi = (v/f)^2$. The bulk gauge symmetry $SO(5) \times U(1)_X \times SU(3)$ is broken down to the SM gauge group on the ultraviolet (UV) boundary and to $SO(4) \times U(1)_X \times SU(3)$ on the infrared (IR). With the symmetry-breaking pattern of the bulk and IR boundary given by $SO(5) \rightarrow SO(4)$ we have four Goldstone bosons parametrized by the $SO(5)/SO(4)$ coset. In this paper we will work in the framework of the minimal models presented in Refs. [21, 22]. With mild tuning, they are consistent with electroweak precision tests (EWPT). The electroweak symmetry is broken dynamically via top loop effects. The Higgs Yukawa couplings and hence the form of the Higgs potential of the low-energy effective theory depends on the way the SM fermions are embedded in representations of the bulk symmetry. In the minimal composite Higgs model MCHM4 [21] the SM fermions transform as spinorial representations of $SO(5)$ whereas in the MCHM5 model [22] as fundamental representations. The Higgs potential is generated at one loop by gauge and fermion interactions.

¹A direct probe is provided by the production of heavy resonances of the strong sector. Further tests are given by the observation of longitudinal gauge boson scattering growing with the energy or strong double Higgs production in longitudinal gauge boson fusion [6]. See also Ref. [13] for a probe of EWSB.

²In Ref. [19] a study of Higgs self-interactions was performed in the context of genuine dimension-six operators. Sensitivities were, however, derived for e^+e^- linear colliders.

In MCHM4, it is given by

$$V(h) = \alpha \cos \frac{h}{f} - \beta \sin^2 \frac{h}{f}, \quad (1)$$

where α, β are integral functions of the form factors in the low-energy effective Lagrangian encoding the effect of the strong dynamics. EWSB is triggered by the top loops, and the Higgs field h acquires a vacuum expectation value (VEV) v defined by

$$v \equiv f\sqrt{\xi} = f \sin \frac{\langle h \rangle}{f} = 246 \text{ GeV}. \quad (2)$$

Expanding the Higgs potential around the VEV we can read off directly the trilinear and quartic Higgs self-couplings from

$$V(H) = V(\langle h \rangle) + \frac{1}{2}M_H^2 H^2 + \frac{1}{6}\sqrt{1-\xi} \lambda_{H^3}^{\text{SM}} H^3 + \frac{1}{24} \left(1 - \frac{7}{3}\xi\right) \lambda_{H^4}^{\text{SM}} H^4, \quad (3)$$

where we have introduced the SM trilinear and quartic Higgs couplings

$$\lambda_{H^3}^{\text{SM}} = \frac{3M_H^2}{v} \quad \text{and} \quad \lambda_{H^4}^{\text{SM}} = \frac{3M_H^2}{v^2}. \quad (4)$$

The mass squared of the Higgs field fluctuation H around the minimum is given by

$$M_H^2 = \frac{4\beta^2 - \alpha^2}{2\beta f^2}. \quad (5)$$

The potential Eq. (1) can get further contributions from additional heavy fields [21], but they will not change the trilinear Higgs coupling. In MCHM5, the Higgs potential reads

$$V(h) = \sin^2 \frac{h}{f} \left(\alpha - \beta \cos^2 \frac{h}{f} \right). \quad (6)$$

Expansion around the VEV leads to

$$V(H) = V(\langle h \rangle) + \frac{1}{2}M_H^2 H^2 + \frac{1}{6} \left(\frac{1-2\xi}{\sqrt{1-\xi}} \right) \lambda_{H^3}^{\text{SM}} H^3 + \frac{1}{24} \left(\frac{3-28\xi(1-\xi)}{3(1-\xi)} \right) \lambda_{H^4}^{\text{SM}} H^4 \quad (7)$$

where

$$M_H^2 = \frac{2(\beta^2 - \alpha^2)}{\beta f^2}. \quad (8)$$

As can be inferred from Eqs.(3) and (7) the trilinear and quartic Higgs couplings depend on the mass of the Higgs boson and the parameter ξ . This is different from the SM, where they are uniquely determined by the mass of the Higgs boson. The Higgs couplings to fermions and gauge bosons are also modified compared to the SM couplings by corrections of the order ξ . The modification factors of the interactions relevant for our analysis are summarized in Table 1 for MCHM4 and MCHM5.

Whereas in both models the Higgs gauge couplings are always reduced compared to the SM, in MCHM5 this is not the case for the trilinear Higgs and the Higgs couplings to fermions. Near the SM limit for low values of ξ these couplings are reduced, with a stronger reduction in MCHM5 than in MCHM4, but for large values of ξ the couplings in MCHM5 rise again and can become

Model/Coupling	HVV	$HHVV$	Hff	HHH
MCHM4	$\sqrt{1-\xi}$	$1-2\xi$	$\sqrt{1-\xi}$	$\sqrt{1-\xi}$
MCHM5	$\sqrt{1-\xi}$	$1-2\xi$	$\frac{1-2\xi}{\sqrt{1-\xi}}$	$\frac{1-2\xi}{\sqrt{1-\xi}}$

Table 1: The Higgs couplings to massive gauge bosons $V = Z, W^\pm$, to fermions f and the trilinear Higgs self-coupling with respect to the SM couplings in MCHM4 and MCHM5 [6, 10].

much larger than in the SM. The couplings can even vanish in this model (for $\xi = 0.5$). This will significantly affect all Higgs production processes involving Higgs fermion couplings. Despite the vanishing Higgs couplings to fermions the fermion masses are still created by the Higgs mechanism, since the direct coupling to the VEV is non-zero.

A novel coupling which is relevant for our analysis is the direct coupling of two Higgs bosons to two fermions. It is suppressed by another power of v compared to the SM Higgs Yukawa coupling and is given by

$$\text{MCHM4:} \quad HHff : \xi \frac{m_f}{v^2} \quad (9)$$

$$\text{MCHM5:} \quad HHff : 4\xi \frac{m_f}{v^2}. \quad (10)$$

In the SM limit, $\xi = 0$, it vanishes as expected.

Before we turn to our analysis a comment on the constraints on ξ from direct searches at LEP and Tevatron as well from indirect constraints due to electroweak precision measurements is at order.³ The direct search at LEP excludes $\xi \approx 0.7 - 0.95$ for M_H ranging from ~ 115 to 80 GeV. Low ξ values are excluded by the Tevatron search for $M_H \approx 162 - 167$ GeV. In MCHM5 an additional region for large ξ values ranging from $\sim 110 - 200$ GeV is excluded.

Concerning the EW precision data, in composite models there are three main contributions to the oblique parameters [23]. The contribution to the T parameter would impose a very large compositeness scale f . If we assume, however, the custodial symmetry to be preserved by the strong sector, there is no contribution to the T parameter. The models which we consider fulfill this requirement. The contribution to the S parameter imposes a lower bound on the mass of the heavy resonances, $m_\rho \gtrsim 2.5$ TeV. We assume the mass gap between the Higgs boson and the strong sector resonances to be large enough to fulfill this constraint. Finally, since the Higgs couplings to the SM gauge bosons are altered by corrections of the order ξ the cancellation between the Higgs and gauge boson contributions to S and T does not hold anymore in contrast to the SM case. They are hence both logarithmically divergent [24].⁴ This leads to an upper bound on the compositeness parameter of $\xi \lesssim 0.2 - 0.4$ in the Higgs mass range $M_H = 80 - 200$ GeV [25]. This bound can be relaxed by about a factor 2, if we allow for a partial cancellation of the order of 50% with contributions from other states [10].

³See Ref. [10] for details.

⁴If the strong sector is invariant under custodial symmetry, the divergence in T will be finally screened by the heavy resonances.

Perturbative requirements forbid the limit $\xi \rightarrow 1$, especially for MCHM5. A rough estimate shows that values close to 1 are allowed. The exact limit depends on the details of the models.

3 Higgs Pair Production Processes

The Higgs potential is determined by the mass of the physical Higgs boson and the trilinear and quartic Higgs self-couplings. In the composite Higgs models the Higgs self-interactions are given by M_H and ξ , *i.e.* for λ_{HHH} ,

$$\text{MCHM4:} \quad \lambda_{HHH} = \sqrt{1-\xi} \lambda_{HHH}^{SM} \quad (11)$$

$$\text{MCHM5:} \quad \lambda_{HHH} = \frac{(1-2\xi)}{\sqrt{1-\xi}} \lambda_{HHH}^{SM}, \quad (12)$$

with the SM trilinear coupling being uniquely determined by M_H . Through the measurement of λ_{HHH} we make a first step towards a full reconstruction of the Higgs potential and gain insights in the dynamics at the origin of EWSB. A departure from the SM relation between Higgs boson mass and Higgs self-couplings would indicate New Physics beyond the SM.

The trilinear Higgs coupling can be measured directly in the production of a pair of Higgs bosons. At the LHC, Higgs pairs can be produced through double Higgs-strahlung off W and Z bosons [26], WW and ZZ fusion [27], and gluon gluon fusion [28]. In principle, the cross sections in the composite Higgs model can easily be derived from the SM cross sections by multiplying the SM Higgs couplings with the corresponding modification factors, cf. Table 1. There is one caveat, however. In gluon fusion to a Higgs boson pair there is an additional diagram, which vanishes in the SM limit and which involves the direct coupling of a pair of Higgs bosons to two fermions. It is shown as the last diagram in gg double Higgs fusion in Fig. 1, which displays the generic diagrams contributing to the Higgs pair production processes at the LHC. The trilinear Higgs coupling is marked by a blob in the different processes.

The parton cross sections for double Higgs-strahlung WHH and ZHH have been obtained from the corresponding results for e^+e^- collisions [29] by adjusting the couplings properly and taking into account the modification of the composite Higgs couplings with respect to the SM case. The gluon fusion cross section has been derived from Ref. [30] by implementing the appropriate correction factors of order ξ in the Higgs interactions and by adding the new diagram. This has been cross checked in a second independent calculation. The production processes at the LHC are then obtained by folding the double Higgs production parton cross sections of the quark and gluon subprocesses, respectively, $\hat{\sigma}(gg/qq' \rightarrow HH; \hat{s} = \tau s)$ with the corresponding luminosities $d\mathcal{L}^{gg/qq'}/d\tau$,

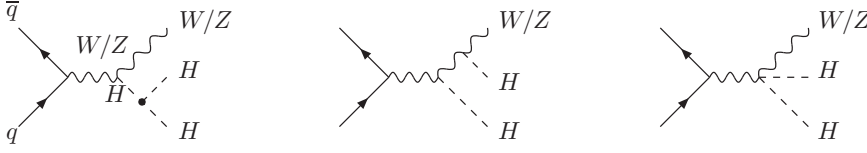
$$\sigma(pp \rightarrow HH) = \int_{\tau_0}^1 d\tau \frac{d\mathcal{L}^{gg/qq'}}{d\tau} \hat{\sigma}(gg/qq' \rightarrow HH + X; \hat{s} = \tau s) \quad (13)$$

with

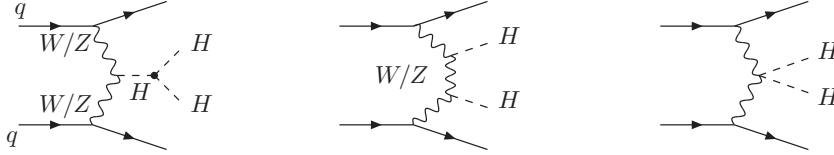
$$\frac{d\mathcal{L}^{gg/qq'}}{d\tau} = \int_{\tau}^1 \frac{dx}{x} f^{g/q}(x; Q^2) f^{g/q'}(\tau/x; Q^2), \quad (14)$$

where $f^{g/q^{(\prime)}}$ denote the quark and gluon parton densities in the proton at a typical scale Q . We have taken $Q = \sqrt{\hat{s}}$ in gluon fusion, $Q = \sqrt{(M_V + 2M_H)^2}$ in Higgs-strahlung and $Q = M_V$

double Higgs-strahlung: $q\bar{q} \rightarrow ZHH/WHH$



WW/ZZ double Higgs fusion: $qq \rightarrow qqHH$



gg double Higgs fusion: $gg \rightarrow HH$

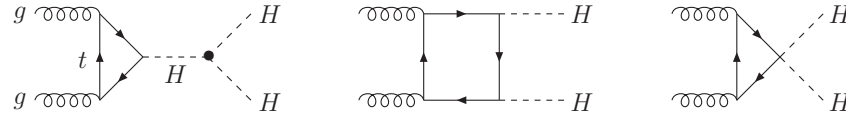


Figure 1: Generic diagrams of the Higgs pair production processes at the LHC in the composite Higgs model: double Higgs-strahlung, WW/ZZ fusion and gg fusion.

($V = W, Z$) in the gauge boson fusion processes. The kinematic threshold is denoted by τ_0 , *i.e.* $\tau_0 = 4M_H^2/s$ in gluon and gauge boson fusion and $\tau_0 = (M_V + 2M_H)^2/s$ in Higgs-strahlung. The double gauge boson fusion cross sections have been calculated with Madgraph/Madevent [31] after implementing the composite Higgs model.

Figure 2 shows the double Higgs production processes as a function of the Higgs mass $M_H = 80 - 200$ GeV in the SM and compared to the composite Higgs boson cross sections for MCHM4 and three representative values of $\xi = 0.2, 0.5, 0.8$. The corresponding plots for MCHM5 are displayed in Fig. 3. Throughout the whole paper we assume a center-of-mass energy of 14 TeV, and we have adopted the parton distribution functions CTEQ6L1 [32].

As can be inferred from the figures, in the SM the gluon fusion process is by far dominant due to the large number of gluons in high-energy proton beams. In view of the results for single Higgs production [33], QCD radiative corrections are expected to be important for this channel. In the low-energy limit for small Higgs masses $M_H^2 \ll 4M_t^2$ they lead to a K factor of $K \approx 2$ [15] in the mass range considered here. Since the QCD corrections of the SM can be translated in a straightforward way to our composite Higgs model they have been included in the plots.

The next important processes are given by the sum of WW and ZZ fusion, with the WW fusion channel dominating over ZZ fusion by a factor $\sim 2.2 - 2.8$ for $\xi = 0 - 0.8$. Double Higgs-strahlung provides the smallest cross sections due to the scaling behaviour $\sim 1/\hat{s}$. The cross sections for WHH and ZHH have been summed with WHH being larger by $\sim 1.6 - 2.1$ for $\xi = 0 - 0.8$. The vertical arrows in the figures show the change of the cross sections for a variation of the Higgs

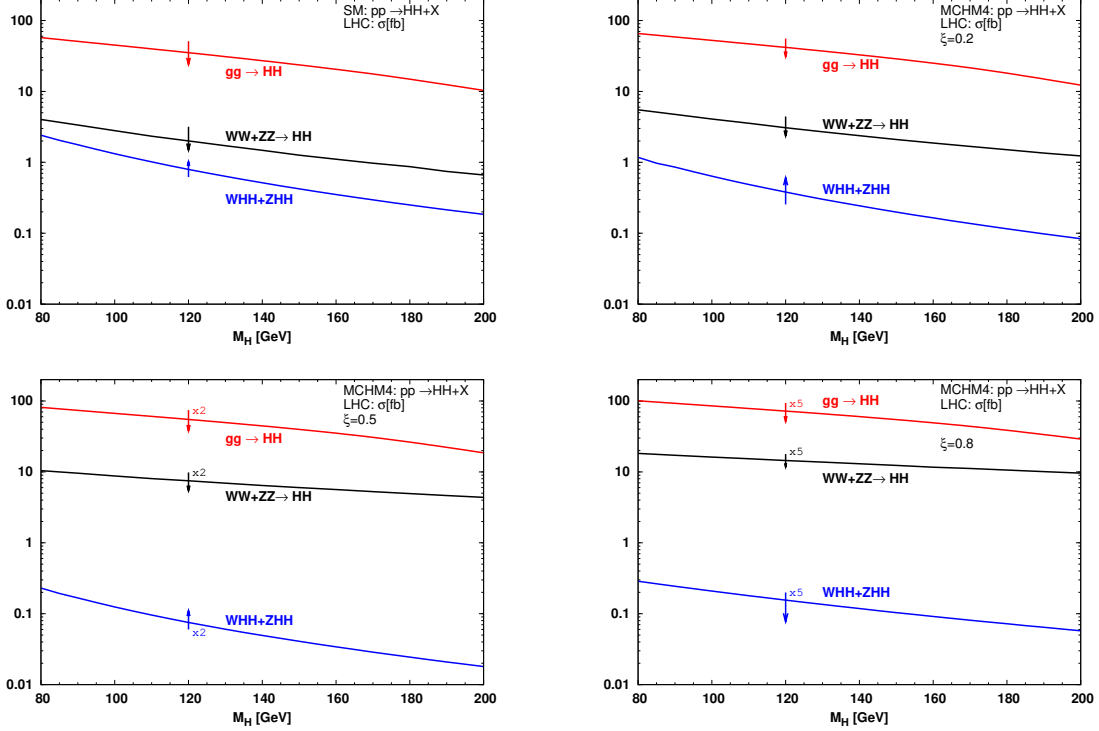


Figure 2: Higgs pair production processes as a function of the Higgs boson mass in the SM ($\xi = 0$, upper left) and MCHM4 with $\xi = 0.2$ (upper right), 0.5 (bottom left) and 0.8 (bottom right). Arrows indicate the change in the cross section for a variation of λ_{HHH} from 0.5 to 1.5 its value in the corresponding model.

self-coupling from 0.5 to 1.5 times its value in the corresponding model, *i.e.* with $\kappa \in [0.5 \dots 1.5]$ ⁵

$$\begin{aligned}
 \lambda'_{HHH} &= \kappa \lambda_{HHH}^{\text{SM}} && \text{for the SM} \\
 \lambda'_{HHH} &= \kappa \sqrt{1 - \xi} \lambda_{HHH}^{\text{SM}} && \text{for MCHM4} \\
 \lambda'_{HHH} &= \kappa \frac{1 - 2\xi}{\sqrt{1 - \xi}} \lambda_{HHH}^{\text{SM}} && \text{for MCHM5.}
 \end{aligned} \tag{15}$$

They indicate the sensitivity to λ_{HHH} in the different models. Where necessary amplification factors have been applied for the arrows to make them visible in the plots.

The size of the composite Higgs pair production cross sections with varying ξ as well as their sensitivity to λ_{HHH} can be understood by examining the interference structure of the contributing diagrams and the size and sign of the composite Higgs couplings. In interpreting the gluon fusion cross section the additional new diagram due to the direct Higgs pair coupling to $q\bar{q}$ has to be taken into account. We start the discussion with

gg Fusion: Due to the diagrams involving the $HHq\bar{q}$ coupling the cross section increases with rising ξ . The larger $HHq\bar{q}$ coupling in MCHM5 leads to a more important increase than in MCHM4. The cross section can be up to a factor 30 bigger than in the SM with values of $\mathcal{O}(1 \text{ pb})$. In MCHM4, the sensitivity gets smaller with rising ξ due to the dominance of the $HHq\bar{q}$ diagram and the decreasing Higgs self-coupling. This also holds for MCHM5 and $\xi < 0.5$. The downwards

⁵The starting (end) point of the arrows corresponds to $\kappa = 0.5$ (1.5).

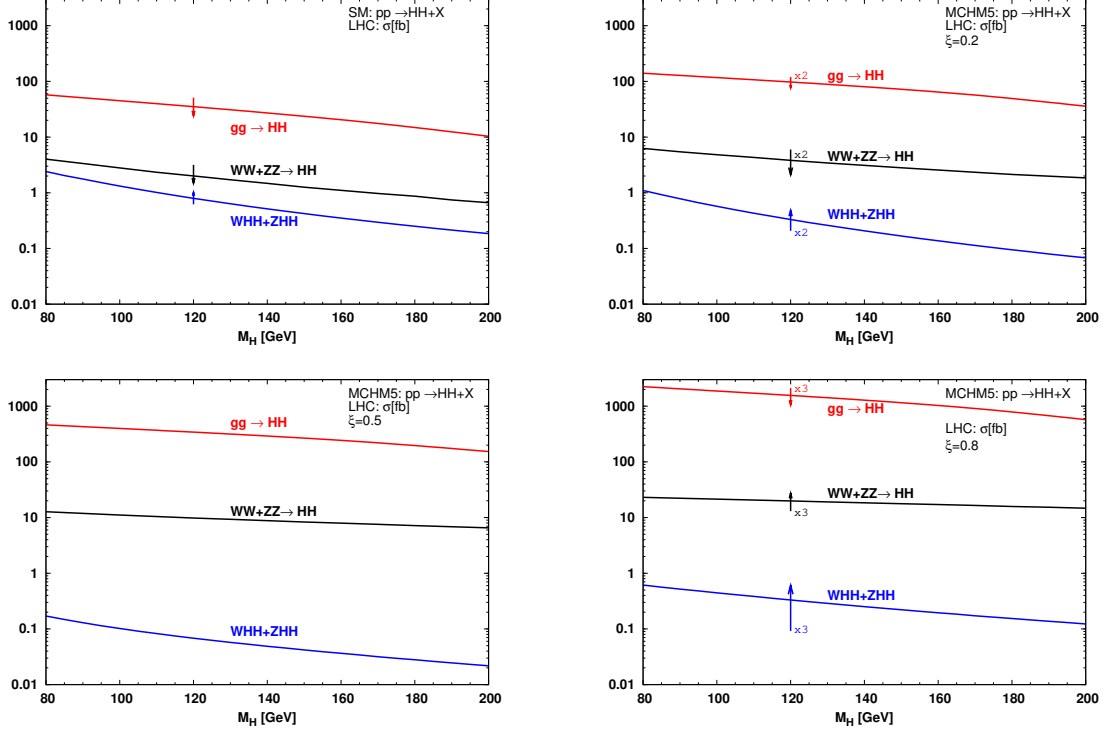


Figure 3: The same as in Fig.2, but for MCHM5.

orientation of the arrows is due to destructive interferences. In MCHM5, at $\xi = 0.5$ the sensitivity completely vanishes since $\lambda_{HHH} = 0$.⁶ Although beyond $\xi = 0.5$ the trilinear Higgs self-coupling in MCHM5 increases with rising ξ , the sensitivity does not, since it is diluted by the more important contribution from the diagram with the $HHq\bar{q}$ coupling, which does not suffer from a suppression due to the Higgs boson propagator.

WW/ZZ Fusion: The vector boson fusion cross section increases with rising ξ but not as much as gg fusion, so that with at most ~ 20 fb it reaches about 5 times the SM cross section. For $\xi \leq 0.5$ the rise is due to the destructive interference of the diagram involving the $VVHH$ coupling with the u - and t - channel diagrams, which gets smaller with the decreasing Higgs gauge couplings in both models. Above $\xi = 0.5$ the $VVHH$ coupling changes sign and the interference becomes constructive leading to larger cross sections. Since in MCHM5 also the λ_{HHH} coupling changes sign above $\xi = 0.5$, the related previously destructive interference becomes constructive and the arrow changes its orientation.

The suppression of the sensitivity to the trilinear coupling with rising ξ is due to the increasing dominance of the strong sector: In the scattering amplitude of the longitudinal gauge bosons the modified Higgs couplings to gauge bosons lead to an incomplete cancellation of the diagrams, which only involve Higgs gauge couplings and which grow with the c.m. energy s . Thus in composite Higgs models double Higgs production in $W_L W_L$ fusion becomes strong [5, 6]. This behaviour can be inferred from the explicit formula of the amplitude for longitudinal gauge boson scattering in a

⁶A similar behaviour is found *e.g.* in the MSSM where the triple Higgs couplings vanish for certain choices of the parameter space, *cf.* Ref. [14, 29].

pair of Higgs bosons,

$$\begin{aligned} \mathcal{M} &= G_F \frac{s}{\sqrt{2}} \left\{ (1 + \beta_W^2) \left[(1 - 2\xi) + \frac{A \cdot \lambda_{HHH}^{\text{SM}}}{(s - M_H^2)/M_Z^2} \right] \right. \\ &\quad \left. + \frac{1 - \xi}{\beta_W \beta_H} \left[\frac{(1 - \beta_W^4) + (\beta_W - \beta_H \cos \theta)^2}{\cos \theta - x_W} - \frac{(1 - \beta_W^4) + (\beta_W + \beta_H \cos \theta)^2}{\cos \theta + x_W} \right] \right\} \\ &\xrightarrow{s \rightarrow \infty} -\sqrt{2} G_F s \xi, \end{aligned} \tag{16}$$

with $\beta_{W,H}$ denoting the W, H velocities and θ the Higgs production angle in the c.m. frame of WW , and $x_W = (1 - 2M_H^2/s)/(\beta_W \beta_H)$. We have $A = 1 - \xi$ in MCHM4 and $A = 1 - 2\xi$ in MCHM5. The high-energy limit agrees exactly with the behaviour of the longitudinal gauge boson scattering amplitude given in Refs. [5, 6].

Both in gg and WW fusion for high energies the diagrams without λ_{HHH} will hence completely dominate and dilute the sensitivity to λ_{HHH} . The distribution in the invariant mass of the Higgs pair, which is sensitive to λ_{HHH} [16–18], can then only be exploited in the region close to the threshold to get access to the trilinear Higgs coupling [6].⁷

WHH/ZHH : In the SM all diagrams interfere constructively. For non-vanishing $\xi < 0.5$ all composite Higgs couplings are suppressed compared to the SM so that the cross sections in MCHM4 and 5 are less important. For $\xi > 0.5$, the $HHVV$ coupling changes sign, and in MCHM4 the diagram interferes destructively with the one involving λ_{HHH} . The cross section increases with rising ξ , *i.e.* smaller Higgs self-coupling, and the arrow changes orientation. In MCHM5, also the trilinear Higgs coupling changes sign and the interference between the two diagrams remains constructive. For small ξ values the sensitivity is larger in MCHM4, since λ_{HHH} is bigger than in MCHM5. For large values of ξ , λ_{HHH} is larger in MCHM5 and thus the sensitivity, too. The cross sections are small and do hardly exceed 1 fb in the composite Higgs models.

4 Sensitivities

In this section we will discuss the sensitivity of the Higgs pair production cross sections to the trilinear Higgs coupling. We will ask two questions:

- 1.) What are the prospects to distinguish composite Higgs pair production from the SM case?
- 2.) What are the prospects to extract the trilinear composite Higgs coupling from the double Higgs production processes?

We will investigate these questions by constructing sensitivity areas for various final states. The final states are dictated by the Higgs branching ratios. These depend on the mass of the Higgs boson and the value of ξ . Since in MCHM4 the Higgs couplings to a pair of gauge bosons and fermions are modified by the same factor, the branching ratios do not change with respect to the SM [6, 10]. These are shown as a function of the Higgs boson mass in Fig. 4. They have been obtained by means of the program HDECAY [34]. As can be inferred from the figure, for M_H below the gauge boson threshold the Higgs boson dominantly decays into $b\bar{b}$. Above ~ 140 GeV the main decay channel is given by the W^+W^- final state, followed by ZZ . Figures 5 show the

⁷We thank Christophe Grojean for drawing our attention to this point.

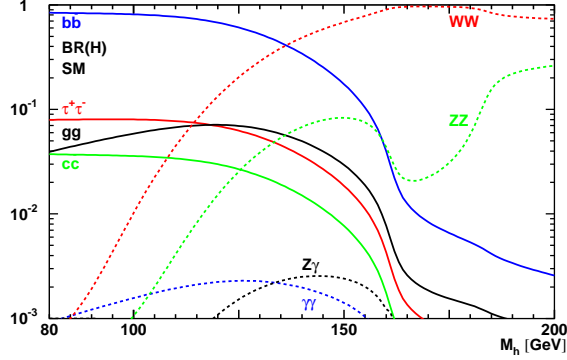


Figure 4: The branching ratios in the SM and MCHM4 as a function of M_H .

branching ratios in MCHM5 as function of ξ for two values of $M_H = 120$ and 180 GeV.⁸ The SM limit corresponds to $\xi = 0$ in Figs. 5. In MCHM5, the behaviour can be drastically different from the SM. For Higgs masses below the gauge boson threshold and small values of ξ , the Higgs boson dominantly decays into $b\bar{b}$, as in the SM. For $\xi = 0.5$, however, where the coupling to fermions vanishes⁹, the decays into gauge bosons dominate and the rare decay into a clean final state photon pair can be as large as a few percent. Above the gauge boson threshold the decays are dominated by W^+W^- and ZZ final states up to near the technicolor limit, where the Higgs gauge couplings are very small and the Higgs fermion couplings are enhanced, so that the decay into $b\bar{b}$ is the most important one.

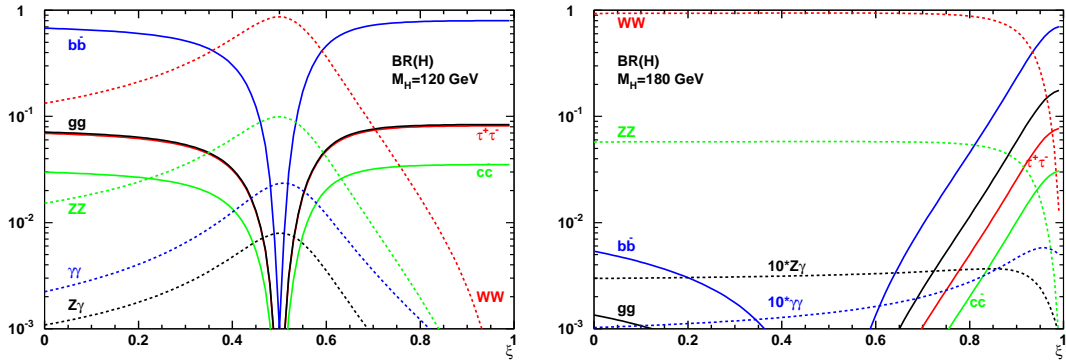


Figure 5: The branching ratios in MCHM5 as a function of ξ for $M_H = 120$ GeV (left) and $M_H = 180$ GeV (right) [10].

For the production processes we concentrate on gg fusion. In gauge boson fusion the additional two tagging jets could be exploited. However, the cross section is an order of magnitude smaller than

⁸ For the generation of the branching ratios the Higgs coupling modifications in MCHM5 have been implemented in the program HDECAY [34].

⁹The Higgs boson decay into fermions through electroweak particle-loops cannot compete with the loop-mediated $\gamma\gamma$ decay, since it has in addition to the loop suppression factor a suppression factor of order m_f^2/M^2 where m_f is the light fermion mass and M is a mass of electroweak size that can be either the Higgs mass, the top mass or the W mass depending on the diagram involved. The decay is about 2 orders of magnitude subdominant compared to the $\gamma\gamma$ decay [10].

gg fusion. The Higgs radiation cross sections, too, are too small to be accessible. The smallness of the Higgs pair production cross section and the large backgrounds represent a considerable challenge. For Higgs boson masses below the gauge boson threshold the decay into $b\bar{b}$ has to be combined with a rare decay of the second Higgs boson, since the $4b$ final state is hopeless in view of the huge QCD background. We therefore investigate the $b\bar{b}\gamma\gamma$ and the $b\bar{b}\tau\tau$ final states. For Higgs masses above ~ 140 GeV, the $4W$ final state is most promising. We first address the question:

1.) Can composite Higgs pair production be distinguished from the SM case?

In order to get a compact answer we have constructed sensitivity areas in the $\xi - M_H$ plane. For each Higgs mass we have determined the value of ξ where the Higgs pair production cross section with subsequent decay in the different final states deviates by more than 1, 2, 3 or 5σ from the corresponding SM process. Denoting by S^{MCHM} the number of signal events for the process calculated in the composite Higgs model and by S^{SM} the corresponding number in the SM, there is sensitivity if

$$S^{\text{SM}} + \beta \sqrt{S^{\text{SM}}} > S^{\text{MCHM}} \quad \text{or} \quad S^{\text{SM}} - \beta \sqrt{S^{\text{SM}}} < S^{\text{MCHM}} \quad (\beta = 1, 2, 3, 5). \quad (17)$$

We assumed an integrated luminosity of 300 fb^{-1} . The results are presented in Fig. 6 and in Fig. 7 for MCHM4 and MCHM5, respectively. The sensitivity areas are shown for the final states $b\bar{b}\gamma\gamma$, $b\bar{b}\tau\tau$ and $W^+W^-W^+W^-$. For comparison we also show $b\bar{b}\mu^+\mu^-$. The sensitivity areas are a result of an interplay of the production process and the Higgs branching ratios.

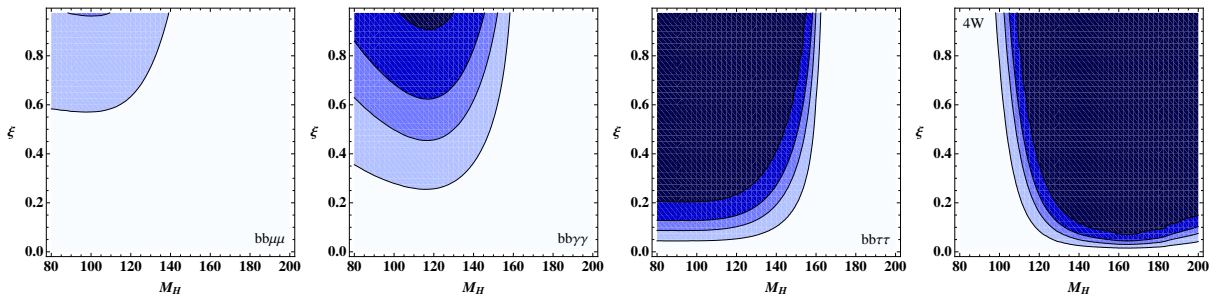


Figure 6: Areas in the $\xi - M_H$ plane, where in the framework of MCHM4 the gluon fusion production of a Higgs pair with subsequent decay deviates from the SM. From dark blue (dark gray) to fair blue (fair gray) the regions corresponds to 5, 3, 2 and 1σ . The final states are from left to right $b\bar{b}\mu^+\mu^-$, $b\bar{b}\gamma\gamma$, $b\bar{b}\tau^+\tau^-$, $4W$, and $\int \mathcal{L} = 300 \text{ fb}^{-1}$.

In MCHM4, *c.f.* Fig. 6, the deviation from the SM is exclusively dictated by the behaviour of the production process, as the MCHM4 branching ratios are the same as in the SM. In the $b\bar{b}\gamma\gamma$ final state, MCHM4 can be distinguished from the SM at 3σ starting from $\xi \approx 0.6$ and for $M_H \lesssim 140$ GeV. Here on the one hand the gluon fusion cross section and on the other hand the branching ratios are large enough to yield the necessary number of signal events. The same holds for the $b\bar{b}\tau\tau$ final state where due to the larger branching ratio in a τ pair the 5σ sensitivity region extends to values of ξ as low as ~ 0.2 for $M_H \lesssim 120$ GeV. In the $4W$ final state the complementary Higgs mass region can be covered, *i.e.* at 5σ $M_H \gtrsim 140$ GeV for $\xi \gtrsim 0.1$ ($M_H \gtrsim 110$ GeV for large ξ values).¹⁰ The $b\bar{b}\mu\mu$ final state on the other hand is hopeless due to its small branching ratios.

¹⁰The sensitivity areas for the $4W$ final state will change, once the W boson decays are included, and depend on the final states into which the W bosons decay.

The no-sensitivity regions are a result of too few events. Altogether, in MCHM4 in the whole mass range ξ values above about 0.1 can be tested. As expected, for lower ξ values no sensitivity to deviations from the SM can be reached.

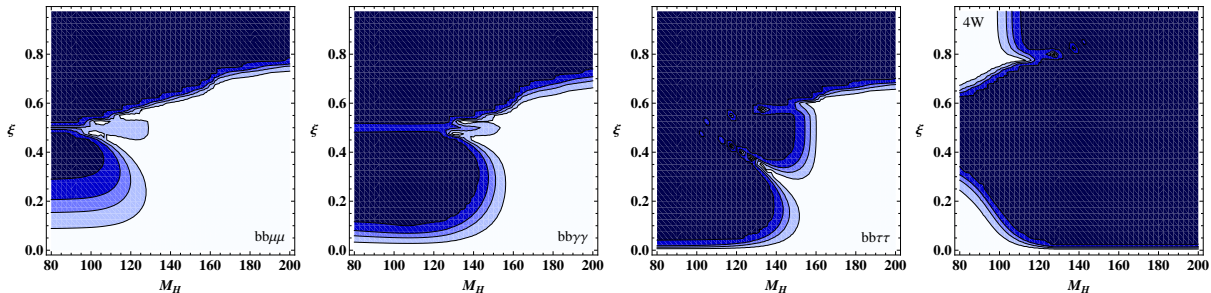


Figure 7: Areas in the $\xi - M_H$ plane, where in the framework of MCHM5 the gluon fusion production of a Higgs pair with subsequent decay deviates from the SM. From dark blue (dark gray) to fair blue (fair gray) the regions corresponds to 5, 3, 2 and 1 σ . The final states are from left to right $b\bar{b}\mu^+\mu^-$, $b\bar{b}\gamma\gamma$, $b\bar{b}\tau^+\tau^-$, $4W$, and $\int \mathcal{L} = 300 \text{ fb}^{-1}$.

In MCHM5, the sensitivity reach in the $\xi - M_H$ parameter space is given by the behaviour of both the Higgs pair production process and the branching ratios. This is why in the $b\bar{b}\mu\mu$, $b\bar{b}\gamma\gamma$, $b\bar{b}\tau\tau$ final states the 5 σ sensitivity areas extend to $M_H \sim 200$ GeV for ξ values above about 0.7 in contrast to MCHM4. This is a result of the large $b\bar{b}$ branching ratio which is important up to high mass values for large ξ , *c.f.* Figs. 5. The vanishing branching ratios into the fermionic final states, however, result in smaller or even vanishing sensitivity areas around $\xi = 0.5$.¹¹ The low-sensitivity regions in the $b\bar{b}\tau\tau$ final state are due to the same reason: The fermionic branching ratios vanish at $\xi = 0.5$. Furthermore, the MCHM5 cross section is larger than the SM one for small and large values of ξ due to the larger production cross section. Therefore there must be regions below and above $\xi = 0.5$ where both the composite Higgs and the SM rates must be the same so that the sensitivity vanishes. With a finer grid in $\xi - M_H$ the disconnected regions of low sensitivity tend to form a connected line extending down to $M_H = 80$ GeV. This behaviour can be clearly seen in the $b\bar{b}\mu\mu$ and $b\bar{b}\gamma\gamma$ final states. The $4W$ final state is sensitive to SM deviations for all ξ values and $M_H \gtrsim 120$ GeV. For small Higgs masses it also covers the difficult region around $\xi = 0.5$ where the branching ratio into W bosons is largely enhanced due to the vanishing $b\bar{b}$ branching ratio. The dots of low sensitivity are the result of an interplay of falling WW branching ratio with rising ξ , see Figs. 5, and a gluon fusion production process which is not yet large enough to make up for it. In summary, in MCHM5 the whole ξ mass range for $\xi \gtrsim 0.05$ can be tested. Compared to MCHM4, the sensitivity areas are larger for the individual final states.

2.) Is there sensitivity to λ_{HHH} in MCHM4 and MCHM5?

Let us now suppose that nature has chosen to realize EWSB in the framework of a composite Higgs model. Furthermore, we assume that the Higgs has been discovered and its couplings to gauge bosons and fermions are known.¹² We want to investigate if a non-zero λ_{HHH} coupling can

¹¹Note that there is non-vanishing sensitivity also for $\xi = 0.5$ because we test here sensitivity to deviations from the SM and not sensitivity to the Higgs self-coupling.

¹² Ref. [35] analyzed the LHC reach in testing deviations from the SM Higgs couplings in the context of composite Higgs models. It was shown that ξ can be extracted with an accuracy of $\mathcal{O}(20\%)$.

be established from the gluon fusion Higgs pair production process so that the Higgs mechanism can be corroborated experimentally. To this goal we derived sensitivity areas in the $\xi - M_H$ parameter space where the cross section with vanishing trilinear Higgs coupling deviates by more than 1, 2, 3 and 5σ at $\int \mathcal{L} = 300 \text{ fb}^{-1}$ from the composite Higgs process with non-zero Higgs self-interaction strength, *i.e.* as given in Eqs. (11,12). They are presented in Fig. 8 and Fig. 9 for MCHM4 and MCHM5. The presented final states are $b\bar{b}\gamma\gamma$, $b\bar{b}\tau\tau$ and $4W$.¹³

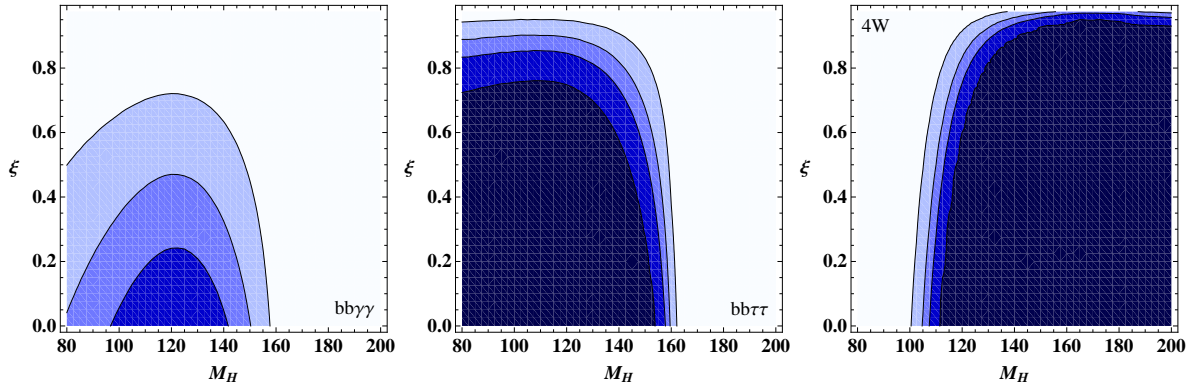


Figure 8: Areas in $\xi - M_H$ with sensitivity to non-vanishing λ_{HHH} in gluon fusion Higgs pair production with subsequent decay for MCHM4. From dark blue (dark gray) to fair blue (fair gray) the regions correspond to 5, 3, 2 and 1 σ . The final states are from left to right $b\bar{b}\gamma\gamma$, $b\bar{b}\tau\tau$, $4W$, and $\int \mathcal{L} = 300 \text{ fb}^{-1}$.

In MCHM4, the contours of the sensitivity areas follow the behaviour of the branching ratios along the M_H direction, *c.f.* Fig. 4. With decreasing importance of the respective branching ratio the sensitivity to non-zero λ_{HHH} drops. In the ξ direction the sensitivity is dominated by the production process. With rising ξ the sensitivity in gluon fusion diminishes, as the diagram with direct coupling of a Higgs to a fermion pair, which is linear in ξ , becomes more and more important. This has been discussed in detail in Section 3. Note that the sensitivity area in the $b\bar{b}\gamma\gamma$ final state where the composite Higgs model can be distinguished from the SM is complementary to the one where a non-zero trilinear Higgs coupling can be established. In the $b\bar{b}\tau\tau$ and $4W$ final states, however, there is considerable overlap of these regions.

In MCHM5, in the $b\bar{b}\gamma\gamma$ and $b\bar{b}\tau\tau$ final states there is sensitivity to λ_{HHH} also for large ξ values up to $M_H = 200 \text{ GeV}$. This is because the fermionic branching ratios stay important up to large Higgs masses for $\xi > 0.5$. For $\xi = 0.5$, however, λ_{HHH} vanishes so that around this value there is no sensitivity at all. In the same final states for low ξ values the sensitivity areas are smaller than in MCHM4, since the trilinear and Yukawa couplings are more strongly suppressed here compared to MCHM4.

Finally, we show in Figs. 10 and 11 the sensitivity to a variation of λ_{HHH} by +30%, *i.e.*

$$\begin{aligned} \lambda'_{HHH} &= 1.3 \sqrt{1 - \xi} \lambda_{HHH}^{\text{SM}} && \text{for MCHM4} \\ \lambda'_{HHH} &= 1.3 \frac{1 - 2\xi}{\sqrt{1 - \xi}} \lambda_{HHH}^{\text{SM}} && \text{for MCHM5.} \end{aligned} \quad (18)$$

¹³We do not show the sensitivity area in the $b\bar{b}\mu\mu$ final state, since it is too small.

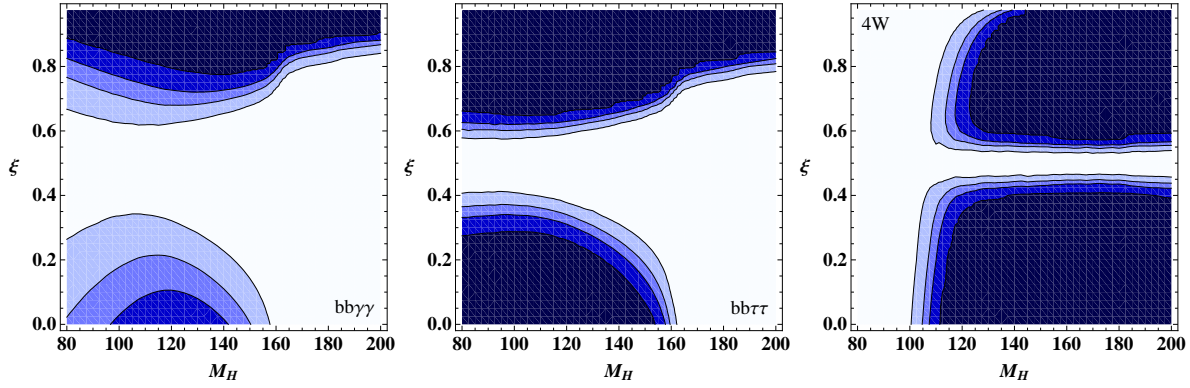


Figure 9: Areas in $\xi - M_H$ with sensitivity to non-vanishing λ_{HHH} in gluon fusion Higgs pair production with subsequent decay for MCHM5. From dark blue (dark gray) to fair blue (fair gray) the regions correspond to 5, 3, 2 and 1 σ . The final states are from left to right $b\bar{b}\gamma\gamma$, $b\bar{b}\tau\tau$, $4W$, and $\int \mathcal{L} = 300 \text{ fb}^{-1}$.

We have chosen an integrated luminosity of 600 fb^{-1} . This corresponds to 3 years of running at the LHC design luminosity with two detectors. As expected the sensitivity regions shrink considerably. Nevertheless, in the $4W$ final state above $\sim 120 \text{ GeV}$ a large part of the ξ range can be covered. For low Higgs masses only the difficult $b\bar{b}\tau\tau$ final state allows for a 30% determination of λ_{HHH} at low ξ values. In the $b\bar{b}\gamma\gamma$ final state the high integrated luminosity of an SLHC with 3000 fb^{-1} would be needed.

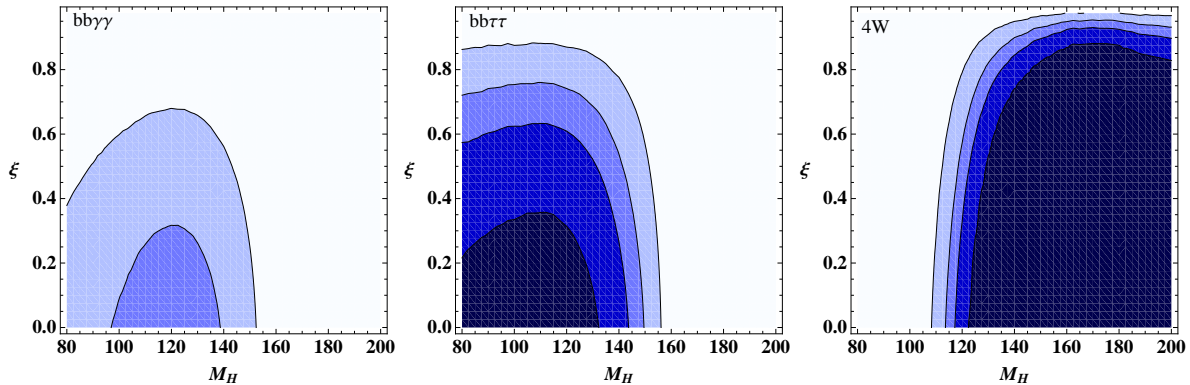


Figure 10: Areas in $\xi - M_H$ with sensitivity to a λ_{HHH} variation of 30% in gluon fusion Higgs pair production with subsequent decay for MCHM4. From dark blue (dark gray) to fair blue (fair gray) the regions correspond to 5, 3, 2 and 1 σ . The final states are from left to right $b\bar{b}\gamma\gamma$ at $\int \mathcal{L} = 3000 \text{ fb}^{-1}$ and $b\bar{b}\tau\tau$, $4W$ at $\int \mathcal{L} = 600 \text{ fb}^{-1}$.

Feasibility: Of course the sensitivity areas shown in Figs. 8-11 represent the ideal case, where we assume that the underlying composite Higgs model has already been pinned down with high accuracy. Furthermore, we assumed the double Higgs production cross sections to be large enough to be measurable. The question arises as to what extent the sensitivity areas will shrink in a full analysis, taking into account the background reactions in a systematic way as well as detector prop-

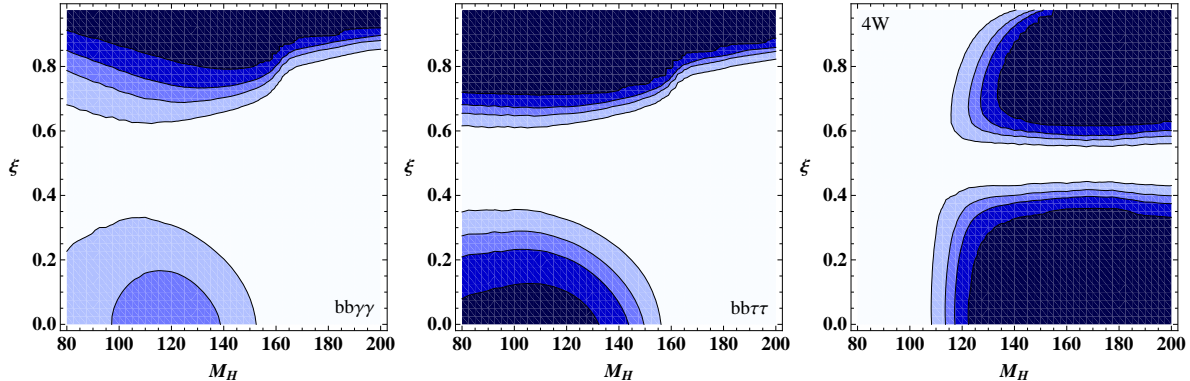


Figure 11: Areas in $\xi - M_H$ with sensitivity to a λ_{HHH} variation of 30% in gluon fusion Higgs pair production with subsequent decay for MCHM5. From dark blue (dark gray) to fair blue (fair gray) the regions correspond to 5, 3, 2 and 1 σ . The final states are from left to right $b\bar{b}\gamma\gamma$ at $\int \mathcal{L} = 3000 \text{ fb}^{-1}$ and $b\bar{b}\tau\tau$, $4W$ at $\int \mathcal{L} = 600 \text{ fb}^{-1}$.

erties.¹⁴ Although this is beyond the scope of this work we can discuss this question qualitatively. As example let us look at the $4W$ final state. In Refs. [17] such an analysis has been performed for the SM Higgs pair production in gluon fusion with subsequent decay of the W boson pairs into four jets and two same-sign leptons, respectively. The main background originates from $W^\pm W^+ W^- jj$ production followed by the $t\bar{t}W^\pm$ background where one top quark decays leptonically, the other hadronically. It has been found that for 300 fb^{-1} a vanishing Higgs self-coupling can be excluded at the 95% CL or better in the mass range 150 to 200 GeV. Furthermore, at the SLHC with 3000 fb^{-1} λ_{HHH} can be determined with an accuracy of 20-30% for $160 \leq M_H \leq 180 \text{ GeV}$. If we look at this in the framework of the composite Higgs model the backgrounds do not change as long as they do not involve any Higgs intermediate state. Such a process would be the subleading electroweak process of Higgs-strahlung off a W boson with subsequent decay into $W^+ W^-$. Since in MCHM4 and MCHM5 the Higgs couplings to gauge bosons are always suppressed compared to the SM we are conservative if we compare to the SM background. A Higgs produced in Higgs-strahlung with subsequent decay into $t\bar{t}$ does not present any danger, since we are well below the top quark pair threshold. As for the signal process in MCHM4 the HH production cross section in gluon fusion with subsequent decay in $4W$ bosons exceeds the SM process for ξ values up to about 0.7. In MCHM5 with an even more enhanced production cross section this regions extends up to ξ close to 1, where it finally vanishes due to zero Higgs couplings to gauge bosons. Combined with our knowledge about the sensitivity areas presented in this section we can conclude that the prospects of excluding vanishing λ_{HHH} or even measuring it with about 30% accuracy are encouraging. If the Higgs mass is below about 140 GeV the situation becomes more difficult. One would have to exploit final states with b -quarks and photons or τ leptons. The extraction of λ_{HHH} is much more difficult here, as has been shown for the SM case in [18]. In MCHM5 we have the additional complication of not being sensitive at all to λ_{HHH} for $\xi \approx 0.5$.

¹⁴For parton level analyses in the SM see Refs. [16–18].

5 Summary

We have systematically investigated the Higgs pair production processes in the minimal composite Higgs models MCHM4 and MCHM5, which give access to the trilinear Higgs self-coupling. A measurement of λ_{HHH} allows to make a first step towards the reconstruction of the Higgs potential. Furthermore, it provides information on the dynamics beyond EWSB. Due to the small cross sections and large backgrounds the measurement is very challenging. For various final states we have constructed areas in the $\xi - M_H$ plane with sensitivity to deviations from the SM as well as sensitivity to a non-vanishing trilinear Higgs self-coupling. As for the $4W$ final state the results are very encouraging and may trigger more sophisticated analyses taking into account all backgrounds and detector effects, which is beyond the scope of this paper.

Acknowledgments

We would like to thank José Espinosa, Christophe Grojean, Tilman Plehn, Michael Rauch, Heidi Rzehak and Michael Spira for helpful discussions. Furthermore, we are grateful to J. Espinosa, Ch. Grojean and M. Spira for the careful reading of the manuscript. This research was supported in part by the Deutsche Forschungsgemeinschaft via the Sonderforschungsbereich/Transregio SFB/TR-9 Computational Particle Physics. MMM would like to thank CERN for kind hospitality where part of this work has been performed.

References

- [1] J. Goldstone, A. Salam and S. Weinberg, Phys. Rev. **127** (1962) 965; S. Weinberg, Phys. Rev. Lett. **19** (1967) 1264; S.L. Glashow, S. Weinberg, Phys. Rev. Lett. **20** (1968) 224; A. Salam, Proceedings Of The Nobel Symposium, Stockholm 1968, ed. N. Svartholm.
- [2] P.W. Higgs, Phys. Lett. **12** (1964) 132; and Phys. Rev. **145** (1966) 1156; F. Englert and R. Brout, Phys. Rev. Lett. **13** (1964) 321; P. W. Higgs, Phys. Rev. Lett. **13** (1964) 508; G.S. Guralnik, C.R. Hagen and T.W. Kibble, Phys. Rev. Lett. **13** (1964) 585.
- [3] For a review see: J.F. Gunion, H.E. Haber, G. Kane and S. Dawson, The Higgs Hunters Guide, Addison-Wesley, 1990; M. Gomez-Bock, M. Mondragon, M. Mühlleitner, R. Noriega-Papaqui, I. Pedraza, M. Spira and P. M. Zerwas, J. Phys. Conf. Ser. **18** (2005) 74 [arXiv:hep-ph/0509077]; M. Gomez-Bock, M. Mondragon, M. Mühlleitner, M. Spira and P. M. Zerwas, arXiv:0712.2419 [hep-ph]; A. Djouadi, Phys. Rept. **457** (2008) 216.
- [4] For a review, see R. Contino, [arXiv:1005.4269 [hep-ph]].
- [5] G. F. Giudice, C. Grojean, A. Pomarol and R. Rattazzi, JHEP **0706** (2007) 045 [hep-ph/0703164].
- [6] R. Contino, C. Grojean, M. Moretti, F. Piccinini and R. Rattazzi, JHEP **1005** (2010) 089. [arXiv:1002.1011 [hep-ph]].
- [7] D. B. Kaplan and H. Georgi, Phys. Lett. B **136** (1984) 183.

- [8] S. Dimopoulos and J. Preskill, Nucl. Phys. B **199**, 206 (1982); T. Banks, Nucl. Phys. B **243**, 125 (1984); D. B. Kaplan, H. Georgi and S. Dimopoulos, Phys. Lett. B **136**, 187 (1984); H. Georgi, D. B. Kaplan and P. Galison, Phys. Lett. B **143**, 152 (1984); H. Georgi and D. B. Kaplan, Phys. Lett. B **145**, 216 (1984); M. J. Dugan, H. Georgi and D. B. Kaplan, Nucl. Phys. B **254**, 299 (1985).
- [9] A. Falkowski, Phys. Rev. D **77** (2008) 055018 [hep-ph/0711.0828].
- [10] J. R. Espinosa, C. Grojean and M. Mühlleitner, JHEP **1005** (2010) 065 [arXiv:1003.3251 [hep-ph]].
- [11] For recent reviews on technicolor models, see C. T. Hill and E. H. Simmons, Phys. Rept. **381** (2003) 235 [hep-ph/0203079]; F. Sannino, hep-ph:0911.0931.
- [12] A. Djouadi, G. Moreau, Phys. Lett. **B660** (2008) 67 [arXiv:0707.3800 [hep-ph]]; G. Bhattacharyya, T. S. Ray, Phys. Lett. **B675** (2009) 222 [arXiv:0902.1893 [hep-ph]]; A. Azatov, M. Toharia, L. Zhu, Phys. Rev. **D82** (2010) 056004 [arXiv:1006.5939 [hep-ph]]; I. Low and A. Vichi, arXiv:1010.2753 [hep-ph].
- [13] E. Accomando, Phys. Lett. **B661** (2008) 129 [arXiv:0709.1364 [hep-ph]].
- [14] A. Djouadi, W. Kilian, M. Mühlleitner and P. M. Zerwas, Eur. Phys. J. C **10** (1999) 45 [arXiv:hep-ph/9904287]; A. Djouadi, W. Kilian, M. Mühlleitner and P. M. Zerwas, arXiv:hep-ph/0001169; M. M. Mühlleitner, arXiv:hep-ph/0008127; M. M. Mühlleitner, arXiv:hep-ph/0101262.
- [15] S. Dawson, S. Dittmaier and M. Spira, Phys. Rev. D **58** (1998) 115012 [arXiv:hep-ph/9805244].
- [16] F. Gianotti *et al.*, Eur. Phys. J. C **39** (2005) 293 [arXiv:hep-ph/0204087]; A. Blondel, A. Clark and F. Mazzucato. ATL-PHYS-2002-029; U. Baur, A. Dahloff, T. Plehn and D. Rainwater in K. A. Assamagan *et al.* [Higgs Working Group Collaboration], arXiv:hep-ph/0406152.
- [17] U. Baur, T. Plehn and D. L. Rainwater, Phys. Rev. Lett. **89** (2002) 151801 [arXiv:hep-ph/0206024]; U. Baur, T. Plehn and D. L. Rainwater, Phys. Rev. D **67** (2003) 033003 [arXiv:hep-ph/0211224].
- [18] U. Baur, T. Plehn and D. L. Rainwater, Phys. Rev. D **68** (2003) 033001 [arXiv:hep-ph/0304015]; U. Baur, T. Plehn and D. L. Rainwater, Phys. Rev. D **69** (2004) 053004 [arXiv:hep-ph/0310056];
- [19] V. Barger, T. Han, P. Langacker, B. McElrath and P. Zerwas, Phys. Rev. D **67** (2003) 115001 [arXiv:hep-ph/0301097].
- [20] R. Contino, Y. Nomura and A. Pomarol, Nucl. Phys. B **671** (2003) 148 [hep-ph/0306259].
- [21] K. Agashe, R. Contino and A. Pomarol, Nucl. Phys. B **719** (2005) 165 [hep-ph/0412089].
- [22] R. Contino, L. Da Rold and A. Pomarol, Phys. Rev. D **75** (2007) 055014 [hep-ph/0612048].
- [23] M. E. Peskin and T. Takeuchi, Phys. Rev. D **46** (1992) 381.

- [24] R. Barbieri, B. Bellazzini, V. S. Rychkov and A. Varagnolo, Phys. Rev. D **76** (2007) 115008 [hep-ph/0706.0432].
- [25] K. Agashe, R. Contino, Nucl. Phys. **B742** (2006) 59-85 [hep-ph/0510164].
- [26] V. D. Barger, T. Han and R. J. N. Phillips, Phys. Rev. D **38** (1988) 2766.
- [27] A. Dobrovolskaya and V. Novikov, Z. Phys. C **52** (1991) 427; D. A. Dicus, K. J. Kallianpur and S. S. D. Willenbrock, Phys. Lett. B **200** (1988) 187; A. Abbasabadi, W. W. Repko, D. A. Dicus and R. Vega, Phys. Rev. D **38** (1988) 2770; Phys. Lett. B **213** (1988) 386.
- [28] E. W. N. Glover and J. J. van der Bij, Nucl. Phys. B **309** (1988) 282.
- [29] A. Djouadi, W. Kilian, M. Mühlleitner and P. M. Zerwas, Eur. Phys. J. C **10** (1999) 27 [arXiv:hep-ph/9903229].
- [30] T. Plehn, M. Spira and P. M. Zerwas, Nucl. Phys. B **479** (1996) 46 [Erratum-ibid. B **531** (1998) 655] [arXiv:hep-ph/9603205].
- [31] J. Alwall *et al.*, JHEP **0709** (2007) 028 [arXiv:0706.2334 [hep-ph]].
- [32] J. Pumplin, D. R. Stump, J. Huston, H.-L. Lai, P. Nadolsky and W.K. Tung, JHEP **0207** (2002) 012. [hep-ph/0201195].
- [33] M. Spira, A. Djouadi, D. Graudenz and P. M. Zerwas, Phys. Lett. B **318** (1993) 347 and Nucl. Phys. B **453** (1995) 17 [arXiv:hep-ph/9504378]; D. Graudenz, M. Spira and P. M. Zerwas, Phys. Rev. Lett. **70** (1993) 1372; S. Dawson, Nucl. Phys. B **359** (1991) 283; A. Djouadi, M. Spira and P. M. Zerwas, Phys. Lett. **B264** (1991) 440; R. P. Kauffman and W. Schaffer, Phys. Rev. D **49** (1994) 551 [hep-ph/9305279]; S. Dawson and R. Kauffman, Phys. Rev. D **49** (1994) 2298 [hep-ph/9310281]; M. Krämer, E. Laenen and M. Spira, Nucl. Phys. B **511** (1998) 523 [hep-ph/9611272]; M. Spira, Fortsch. Phys. **46** (1998) 203 [hep-ph/9705337].
- [34] A. Djouadi, J. Kalinowski and M. Spira, Comput. Phys. Commun. **108** (1998) 56 [hep-ph/9704448]. For an update, see A. Djouadi, J. Kalinowski, M. Mühlleitner and M. Spira in J. M. Butterworth *et al.*, [hep-ph/1003.1643]; A. Djouadi, M. M. Mühlleitner, M. Spira, Acta Phys. Polon. **B38** (2007) 635-644 [hep-ph/0609292].
- [35] S. Bock, R. Lafaye, T. Plehn, M. Rauch, D. Zerwas and P. M. Zerwas, Phys. Lett. B **694** (2010) 44 [arXiv:1007.2645 [hep-ph]].